Available online at www.sciencedirect.com
SCIENCE DIRECT
Journal of Sound and Vibration 295 (2006) 13–27
JOURNAL OF SOUND AND VIBRATION
www.elsevier.com/locate/jsvi

Formulation and validation of boundary conditions at a branched junction for nonlinear waves

Kang Seog Chae[a], Kyung Tae Lee[b], Chang Jeon Hwang[c], Duck Joo Lee[a,*]

[a]*Division of Aerospace Engineering, Department of Mechanical Engineering, Korea Advanced Institute of Science and Technology, 373-1 Guseong-dong, Yusung-gu, Daejeon 305-701, Republic of Korea*
[b]*School of Mechanical and Aerospace Engineering, Sejong University, 98 Gunja-dong, Kwangjin-gu, Seoul 143-747, Republic of Korea*
[c]*Korea Aerospace Research Institute, 45 Eoeun-dong, Yusung-gu, Daejeon 305-333, Republic of Korea*

Received 31 March 2003; received in revised form 27 August 2004; accepted 17 November 2005

Abstract

A numerical model is presented for the calculation of nonlinear waves through the branched junctions in a gas transmission pipe system. In the one-dimensional time domain analysis of the wave dynamics, the behaviour of the nonlinear waves is determined by quasi-steady boundary conditions at junctions in a pipe system. The quasi-steady treatment through the junction yields a system of nonlinear balance equations. The iterative solution procedure of the system of nonlinear equations causes the problems of divergence and multiple solutions. In order to overcome the difficulties, a new set of quasi-linear balance equations is formulated without a sacrifice of accuracy. The present model, therefore, requires a non-iterative solution procedure that results in a unique solution and a smaller computational effort. Thompson's boundary condition is used at each pipe. A new time-derivative form of balance equations, based Thompson' boundary condition, gives a set of linear algebraic equations for the balance equations. When implementing the new time-derivative form of the balance equations, corrected terms are added numerically. The present numerical model is implemented and tested for the calculation of behaviour of nonlinear waves in a branched pipe and the calculation of sound attenuation of a Helmholtz resonator and the prediction of radiated orifice noise of an internal combustion engine. Calculation results show good agreements with previous iterative calculations and measurement data.

1. Introduction

One-dimensional unsteady compressible flow analysis is widely used to predict the wave action phenomena in the gas transmission pipe systems such as the intake and exhaust systems of internal combustion engines, pressure exchangers, and natural gas transport systems. The pipe systems are usually modelled as flow networks, where branched junctions are frequently encountered in the pipe systems. In the numerical calculation of the flow networks, the boundary condition of pipe flows must be implemented at the junctions. The incident, reflection, transmission, and attenuation of pressure waves appear at the junctions. Therefore, an improper specification of the boundary condition contaminates the flows.

*Corresponding author. Tel.: +82 42 869 3716; fax: +82 42 869 3710.
E-mail address: djlee@mail.kaist.ac.kr (D.J. Lee).

0022-460X/$ - see front matter © 2006 Published by Elsevier Ltd.
doi:10.1016/j.jsv.2005.11.023

For the boundary condition of pipe systems, we need additional balance equations for the fluid properties of mass, energy and so on at branched pipe junctions. A quasi-steady flow treatment of balance equations is generally used at the junctions, and the balance equations are coupled with the characteristic information transported from the interior of the pipe to the junction. This information is obtained after solving the interior of the pipe with the boundary conditions of each pipe.

The quasi-steady assumption through the junctions gives the balance equations, which are coupled nonlinear algebraic equations. The characteristic information transported at the boundary of each pipe can be used either with the method of characteristics or the characteristic formulation of the Euler equation. The method of characteristics gives the compatibility condition, which yields the linear algebraic equations with a first-order accuracy. The characteristic formulation of the Euler equation gives a set of ordinary differential equations in time. Then, it is evident that the equations for the boundary condition become either a set of nonlinear and linear algebraic equations [1–7], or a set of nonlinear algebraic equations and ordinary differential equations [8]. Both sets of equations should be solved in an iterative way by means of, for example, the Newton–Raphson method because of the nonlinear balance equations. Although a converged solution may be obtained in the iterative solution procedure, the numerical solution depends on the convergence limit and initial value, and sometimes a non-physical solution can be obtained [5,6].

We have improved the boundary conditions in several ways. Instead of using nonlinear balance equations, we derived a time derivative of the balance equations at the junctions, along with treatment of a correct time-dependent boundary condition for the interior of each pipe. The time derivative of the balance equations become quasi-linear.

For the boundary condition of each pipe, we used the characteristic approach of Thompson's boundary condition [9]. The advantage of this condition is that the time-dependent, incoming and outgoing characteristics of the flow of each pipe can be treated correctly, especially at the junctions where the flows from each branch interact severely. After obtaining this information, we then obtained the time derivative of the flow properties of the density, pressure and velocity. The outgoing information is usually obtained from known properties in the interior of the pipe, but the incoming information from the outside of each pipe should be specified or solved. We use numerical integration in time to calculate the boundary values of the density, pressure and velocity.

A second improvement involves the use of Thompson's characteristic approach. The incoming information is obtained from the balance equations at the junctions of the pipe system. In general, the balance equations are nonlinear and coupled with the boundary condition. We used the time derivative of the density, pressure and velocity in Thompson's boundary condition to reformulate the balance equations into the time-derivative forms. The time derivatives of the balance equations can be arranged as quasi-linear algebraic relations, which do not require an iterative method. To solve the interior of each pipe, the incoming information obtained from the time-derivative forms is then used for Thompson's boundary conditions. The difficulties of divergence and multiple solutions are therefore overcome without loss of accuracy and the computational time is reduced owing to noniterative procedure [5,6].

Finally, in numerically using the time derivative of the balance equations, the balance of mass, energy and so on is imposed at each time step with typical correction terms. Therefore, the problem of initially unbalanced flows can be solved.

2. Mathematical formulation

In this section, we describe the mathematical formulation of the quasi-linear balance equations that govern the flow phenomena through the general n-branch junction. We also discuss the numbers of the unknown boundary values and the necessary equations. To formulate the quasi-linear time-derivative forms of balance equations, we used the time derivatives of the density, pressure and velocity in Thompson's boundary conditions. In this section, we also present the typical correction procedures for the initially unbalanced flow and for the spurious unbalance produced in the numerical calculation of the time-derivative forms.

2.1. Mathematical model

Fig. 1 shows a general n-branch junction where k branches have flow coming into the junction and l branches have flow going out from the junction, obviously satisfying $k+l=n$. Flow through the junction can be modelled by using simplified equations under several assumptions. The equations will be revised to establish a new set of balance equations in the next section.

Firstly, it is assumed that mass accumulation within the junction is negligible. It is also assumed that the mass flow through the branched junction is constant within small time intervals. The assumptions lead to the following quasi-steady balance equations, where the sign convention for particle flows is positive towards the branch:

$$\text{Mass balance}: \sum_{i=1}^{n} \dot{m}_i = 0, \tag{1}$$

$$\text{Energy balance}: \sum_{i=1}^{n} \dot{m}_i h_{oi} = 0, \tag{2}$$

where $\dot{m}$ is mass flow through section area, h_o is total enthalpy, and the subscript, i, denotes the pipe number.

Secondly, it is assumed that the incoming flows become mixed in the junction and, then, the mixed flows are outgoing from the junction with an equal total enthalpy [3,5,6,10]:

$$\text{Equal total enthalpy for outgoing flows}: \quad h_{oi} = h_{ol}, \quad i \in l \text{ but } i \neq l. \tag{3}$$

The global balance of the number of unknown boundary values and the number of necessary equations is essential to obtain a well-posed problem for the quasi-linear formulation of balance equations. For each branch, three boundary values have to be determined and, as a result, the number of boundary values to be solved is $3n$ for the n-branch junction. One can find $2k+l$ physical characteristics transported from the interior of the pipes to the junction for subsonic flows ($2k$ sound and entropy waves for incoming flows and l sound waves for outgoing flows). The conservative law gives two equations, and the equal total enthalpy assumption gives $l-1$ equations. Therefore, $3n-(2k+l)-2-(l-1)=n-1$ equations are required to close the system (see Table 1).

Finally, the pressure relation model can give the further required equations. The simplest model neglects pressure loss in the junction. The model, so-called constant pressure model proposed by Benson [1], is realistic when the flow velocities are low and the entropy levels are almost the same in all branches. Another pressure relation model is based on the momentum equations. The model requires large number of empirical

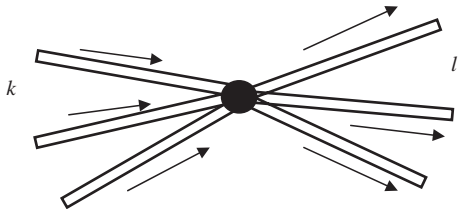

Fig. 1. Schematic of a general n-branch junction.

Table 1
Closure of boundary equations for general n-branch junction ($k+l=n$)

No. of boundary values to be determined	$3n$	Known characteristic wave equations	$2k+l$
		Mass and energy balance equations	2
		Equal total enthalpy assumption	$l-1$
		Pressure loss relation	$n-1$

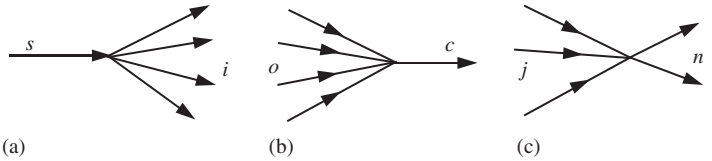

Fig. 2. Classification of an n-branch junction: (a) supplier type; (b) collector type; (c) the other type.

coefficients that are quite difficult to measure [2]. Also, generalization of the model is almost impossible to the general n-branch junction (for $n>3$) [4].

The other sophisticated relation is based on relative pressure losses, where the static pressure loss [2,4,10] or the total pressure loss [5,6] from one branch to another depends on flow velocity and the pressure loss coefficient. Bingham's pressure relation model expresses the static pressure losses dependent on the dynamic head in a downstream pipe and the empirical loss coefficient [2]. The model has been successfully incorporated into isentropic flow calculation [2] and validated with non-isentropic flow analysis [10]. The model is adopted in the present paper, too.

Bingham's model classifies the branched junction into supplier type, collector type, and the other types (see Fig. 2). The pressure relations for the corresponding type are described as follows:

$$\text{For supplier type}: \quad p_s - p_i = \tfrac{1}{2}\rho_i u_i^2 \xi_{si}, \quad i \in l\,, \tag{4a}$$

$$\text{For collector type}: \quad p_o - p_c = \tfrac{1}{2}\rho_c u_c^2 \xi_{oc}, \quad o \in k\,, \tag{4b}$$

$$\text{For the other types}: \quad p_j = p_n, \quad j \in n \text{ but } j \neq n\,, \tag{4c}$$

where p is the pressure, u the flow velocity, ρ the density, and ξ the pressure loss coefficient. The relative pressure loss relation gives the further $n-1$ equation, and then all of required equations are established to close the system (see Table 1).

The difficulties of divergence and multiple solutions in the iterative solution procedure of the nonlinear balance Eqs. (1)–(4) were reported in the previous study, even though to the case of $n=3$ [6]. The relations are coupled with the boundary condition of each pipe. To overcome the difficulties, it was also proposed that the multibranch junction could be decomposed into its superposed 2-branch junctions [6] or 3-branch junctions [4], always solving only 2- or 3-branch junction equations. One of the methods is called the 'branch superposition method' [6]. While it is possible to obtain a numerical robustness by decomposition, the numerical model requires a further iteration procedure, and the convergence of iterative calculation is limited because the set of balance equations is usually over conditioned (the number of necessary equations is larger than that of the unknown boundary values) [4,6].

The balance Eqs. (1)–(4) can be rewritten, for example, for a supplier type 3-branch junction shown in Fig. 3:

$$\text{Mass balance}: \quad \dot{m}_1 + \dot{m}_2 + \dot{m}_3 = 0, \tag{5}$$

$$\text{Energy balance}: \quad \dot{m}_1 h_{o1} + \dot{m}_2 h_{o2} + \dot{m}_3 h_{o3} = 0, \tag{6}$$

$$\text{Equal total enthalpy for outgoing flows}: \quad h_{o2} = h_{o3}, \tag{7}$$

$$\text{Relative pressure losses}: \quad p_1 - p_2 = \tfrac{1}{2}\rho_2 u_2^2 \xi_{12}, \tag{8a}$$

$$p_1 - p_3 = \tfrac{1}{2}\rho_3 u_3^2 \xi_{13}. \tag{8b}$$

2.2. Quasi-linear formulation

In solving the set of nonlinear balance equations, Eqs. (1)–(4), the flow properties of the density, pressure, velocity and enthalpy are coupled with the boundary conditions and the governing equations of each pipe.

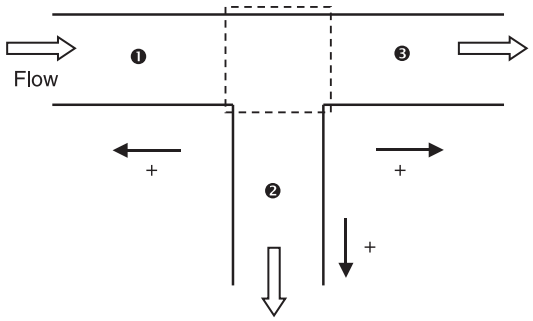

Fig. 3. Schematic of a supplier type 3-branch junction.

Obtaining a linear set or quasi-linear set of balance equations is therefore desirable because difficulties arise in an iterative procedure, as described in the previous section. The time-derivative forms of the balance equations give the quasi-linear equations. We use Thompson's boundary condition to derive the forms after general discussion of the numerical problem and correction in the time-derivative forms of the balance equation.

2.2.1. Problem and correction in time-derivative forms

Instead of the original balance equation, Eq. (1), the mass balance through the branched junction can be described by using the corresponding differential equation:

$$\text{Differential equation for mass balance}: \frac{\partial\left(\sum_{i=1}^{n}\dot{m}_i\right)}{\partial t}=0. \tag{9}$$

The time derivative in Eq. (9) can be approximated by using the following differencing formula:

$$\frac{\partial\left(\sum\dot{m}_i\right)}{\partial t}=\frac{\left(\sum\dot{m}^{j+1}-\sum\dot{m}^{j}\right)}{\delta t}=0, \tag{10}$$

where j labels the time level. The index of summation convention is omitted.

Let us assume that the mass flow is unbalanced at some time level j during the numerical calculation $\left(\sum\dot{m}^{j}\neq 0\right)$. Then Eq. (10) keeps the unbalance at the next time level $j+1$ $\left(\sum\dot{m}^{j+1}\neq 0\right)$. The non-physical unbalance can occur due to both the unbalanced initial condition and the numerical errors during the course of numerical calculation. The unbalance is maintained and it is accumulated at all later times also. Therefore, it is necessary to force the flow to be balanced at the next time level, $\sum\dot{m}^{j+1}=0$, even though the mass flow is unbalanced at the time level j, $\sum\dot{m}^{j}\neq 0$:

$$\frac{\partial\left(\sum\dot{m}_i\right)}{\partial t}=\frac{\left(\sum\dot{m}^{j+1}-\sum\dot{m}^{j}\right)}{\delta t}=\frac{\left(0-\sum\dot{m}^{j}\right)}{\delta t}=-\frac{\sum\dot{m}^{j}}{\delta t}. \tag{11}$$

Eq. (11) is a new mass balance equation, in which the correction term is added in the right-hand side of Eq. (9). The corresponding corrected differential equations for Eqs. (2)–(4) can be obtained in a similar manner.

2.2.2. Thompson's boundary conditions and time-derivative forms of the balance equations

The characteristic information necessary for the solution of the boundary condition is obtained by the method of characteristics [1–7] or the characteristic formulation of the Euler equation [8]. In the method of characteristics, a trace of characteristics is required, and the characteristic value necessary is obtained by linear interpolation between mesh points. Hence, the solution has only first-order accuracy [4]. When the characteristic formulation of the Euler equation is used for the boundary condition, the resulting boundary equations are a coupled system of partial differential equations in time and nonlinear algebraic equations [8]. The set of equations can be solved by a predictor–corrector scheme, for example, with an iterative solution procedure for the nonlinear equations.

In the present study, Thompson's characteristic approach [9] is adopted to consider the transported characteristic information. The summary of Thompson's approach is presented in Appendix A. The key of

Thompson's approach is that the time variation of the boundary value is represented in terms of the time variation of characteristic wave amplitudes. Then, the problem of implementing a boundary condition becomes the problem of finding the unknown characteristic wave amplitudes.

The approach is extended to the boundary condition of a branched junction in the present study. Rearrangement of Eq. (A.10) gives the time derivative of the variables, ρu, h_o, $(1/2)\rho u^2$, $\rho u h_o$, in terms of the variation of characteristic wave amplitudes, R_i. The variables are shown in the balance equations:

$$\frac{\partial(\rho u)}{\partial t}+\frac{1}{a}\left[MR_2+\frac{1}{2}\{(M-1)R_1+(M+1)R_3\}\right]=0, \tag{12}$$

$$\frac{\partial h_o}{\partial t}+\frac{1}{(\gamma-1)\rho}\left[-R_2+\frac{\gamma-1}{2}\{(1-M)R_1+(1+M)R_3\}\right]=0, \tag{13}$$

$$\frac{\partial}{\partial t}\left(\frac{1}{2}\rho u^2\right)+\frac{1}{2}\left[M^2R_2+M\left(\frac{M}{2}-1\right)R_1+M\left(\frac{M}{2}+1\right)R_3\right]=0, \tag{14}$$

$$\frac{\partial(\rho u h_o)}{\partial t}+\frac{a}{2}\left[M^3R_2+(M-1)\left(\frac{M^2}{2}-M+\frac{1}{\gamma-1}\right)R_1+(M+1)\left(\frac{M^2}{2}+M+\frac{1}{\gamma-1}\right)R_3\right]=0, \tag{15}$$

where M is the Mach number and γ the specific heat ratio. The subscript of R denotes the type of characteristic waves.

We derived the above equations to represent the time variations of the balance properties of mass, enthalpy, dynamic pressure and energy in terms of R_i. One of the key points is that the algebraic combinations of R_i can express the time variations of the balance properties. For the new quasi-linear balance equation, we assume the coefficients of R_i are constant at each time during the numerical integration in time.

It is noted that the nonlinear term of variables R_i, such as $\sqrt{R_1}$ and $R_2\,R_3$, is not shown in Eqs. (12)–(15), and the coefficients of R_i do not contain the time derivatives.

We present the new time derivatives of the corrected balance equations in terms of R_i by using Eqs. (12)–(15) as follows. In a supplier type of three-branch junction, for example, by differentiating the time and adding the correction terms, the nonlinear balance equations, Eqs. (5)–(8) become the new quasi-linear simultaneous algebraic balance equations. If the time-derivative terms of the variables ρu, h_o, $(1/2)\rho u^2$, $\rho u h_o$ in Eqs. (12)–(15), are expressed by R_i, at the junction, and on the assumption of constant coefficient of R_i, the new algebraic balance equations (see Eq. (11) for the mass balance) are as follows:

Mass balance :

$$\begin{aligned}&-\left\langle\frac{1}{a}\left[MR_2+\frac{1}{2}\{(M-1)R_1+(M+1)\tilde{R}_3\}\right]A\right\rangle_1-\left\langle\frac{1}{a}\left[M\tilde{R}_2+\frac{1}{2}\{(M-1)R_1+(M+1)\tilde{R}_3\}\right]A\right\rangle_2\\&-\left\langle\frac{1}{a}\left[MR_2+\frac{1}{2}\{(M-1)R_1+(M+1)\tilde{R}_3\}\right]A\right\rangle_3=-\frac{\dot{m}_1^k+\dot{m}_2^k+\dot{m}_3^k}{\delta t},\end{aligned} \tag{16}$$

Energy balance :

$$\begin{aligned}&-\left\langle\frac{a}{2}\left[M^3R_2+(M-1)\left(\frac{M^2}{2}-M+\frac{1}{\gamma-1}\right)R_1+(M+1)\left(\frac{M^2}{2}+M+\frac{1}{\gamma-1}\right)\tilde{R}_3\right]A\right\rangle_1\\&-\left\langle\frac{a}{2}\left[M^3\tilde{R}_2+(M-1)\left(\frac{M^2}{2}-M+\frac{1}{\gamma-1}\right)R_1+(M+1)\left(\frac{M^2}{2}+M+\frac{1}{\gamma-1}\right)\tilde{R}_3\right]A\right\rangle_2\\&-\left\langle\frac{a}{2}\left[M^3\tilde{R}_2+(M-1)\left(\frac{M^2}{2}-M+\frac{1}{\gamma-1}\right)R_1+(M+1)\left(\frac{M^2}{2}+M+\frac{1}{\gamma-1}\right)\tilde{R}_3\right]A\right\rangle_3\\&=-\frac{\dot{m}_1^k h_{o1}^k+\dot{m}_2^k h_{o2}^k+\dot{m}_3^k h_{o3}^k}{\delta t},\end{aligned} \tag{17}$$

Equal total enthalpy for outgoing flows:

$$-\left\langle\frac{1}{\rho}\left[-\frac{R_2}{\gamma-1}+\frac{1}{2}\{(1-M)R_1+(1+M)\tilde{R}_3\}\right]\right\rangle_1+\left\langle\frac{1}{\rho}\left[-\frac{\tilde{R}_2}{\gamma-1}+\frac{1}{2}\{(1-M)R_1+(1+M)\tilde{R}_3\}\right]\right\rangle_2 = -\frac{h_{o1}^k-h_{o2}^k}{\delta t}, \tag{18}$$

Relative pressure losses :

$$-\left\langle\frac{1}{2}(\tilde{R}_3+R_1)\right\rangle_1+\left\langle\frac{1}{2}(\tilde{R}_3+R_1)\right\rangle_2+\frac{1}{2}\xi_{12}\left\langle M^2\tilde{R}_2+M\left(\frac{M}{2}-1\right)R_1+M\left(\frac{M}{2}+1\right)\tilde{R}_3\right\rangle_2 = -\frac{p_1^k-p_2^k-1/2\xi_{12}\rho_2^k u_2^{k^2}}{\delta t}, \tag{19a}$$

$$-\left\langle\frac{1}{2}(\tilde{R}_3+R_1)\right\rangle_3+\left\langle\frac{1}{2}(\tilde{R}_3+R_1)\right\rangle_2+\frac{1}{2}\xi_{32}\left\langle M^2\tilde{R}_2+M\left(\frac{M}{2}-1\right)R_1+M\left(\frac{M}{2}+1\right)\tilde{R}_3\right\rangle_2 = -\frac{p_3^k-p_2^k-1/2\xi_{32}\rho_2^k u_2^{k^2}}{\delta t}, \tag{19b}$$

where A is a section area. The subscript of brace denotes the pipe number (see Fig. 3).

R_i denotes the outgoing property and $\tilde{R}_i$ denotes the incoming property. The outgoing property is known, whereas the incoming property is unknown. The unknowns can be obtained by solving the above system of balance equations, Eqs. (16)–(19).

2.2.3. Procedure for obtaining the boundary values

At any solution condition, the incident characteristic information, which is transported from the interior of the pipe to the boundary, is always known. One can directly obtain the four R_i's of the incident waves, which are the sound and entropy waves of pipe 1 ($\langle R_1\rangle_1$, $\langle R_2\rangle_1$), sound wave of pipe 2 ($\langle R_1\rangle_2$), and sound wave of pipe 3 ($\langle R_1\rangle_3$).

It is assumed that the coefficients of R_i in Eqs. (16)–(19) are locally constant because the coefficients do not contain the time derivatives. Then, the coefficients can be calculated using the values at the time level j, following the Thompson's characteristic approach [9]. The assumption leads to the system of quasi-linear balance equations for the unknown variables. In Eqs. (16)–(19), the tilde marks are placed over the unknowns such as $\tilde{R}_i$. The closed systems of equations are solved in a non-iterative way. After all values of unknowns $\tilde{R}_i$ are set, the time integration of Eq. (A.10) gives the boundary values at the next time level $j+1$.

The one-sided difference evaluation of R_i using Eq. (A.11) can give higher-order accuracy in comparisons with the first-order accuracy of the method of characteristics [4].

3. Numerical validation

The numerical model described in the previous section may be a good tool for predicting wave action phenomena through a branched junction, especially in a complex pipe system for transmitting gas. The model can be also applied to the system of a small pressure fluctuation and a nonlinear wave simulation. We validated the present model by numerically simulating the wave action phenomena in a branched pipe system; the pipe system had a large pressure fluctuation and a simple muffling system with an acoustic harmonic excitation.

3.1. Shock tube with a branched junction

For the first numerical validation of the present boundary condition, the shock tube with a branched junction is considered. The schematic is represented in Fig. 4, where the lengths of pipe are different from each other. The pressure difference between the high- and low-pressure regions is 15 kPa. The low-pressure region is

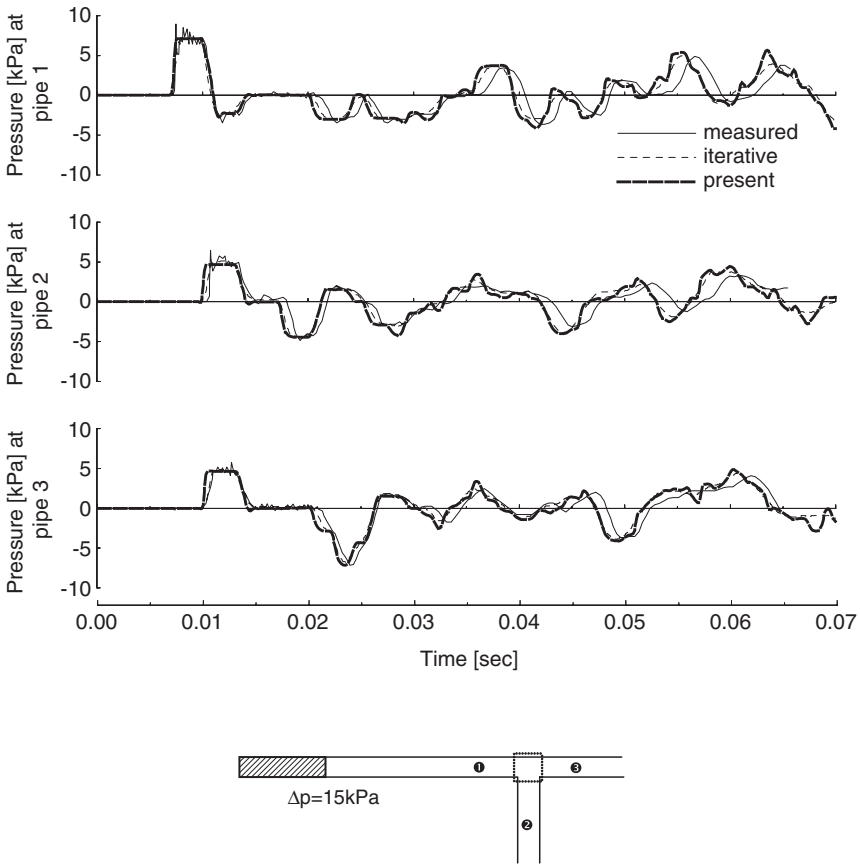

Fig. 4. Pressure history of the shock tube with a 3-branch junction.

initially filled with a quiescent air of ambient condition. William-Louis et al. performed the pressure measurement and an iterative numerical calculation [6]. The method of characteristics is adopted for both the pipe flow calculation and the boundary condition. The 'branch superposition method' is also used for the boundary condition of the branched junction. The method decomposes, as described in the previous section, the branched junction into its superposed 2-branch junctions. Only the balance equations of the superposed 2-branch junction are solved in order to overcome the problems of divergence and multiple solutions.

In the present calculation, the new quasi-linear formulation of balance equations is implemented for the boundary condition. The essentially non-oscillatory (ENO) upwind scheme [11] is applied for pipe flow calculation. For the boundary condition of an open end, the assumptions of a constant atmospheric pressure for outflow and the total energy conservation with an isentropic expansion for inflow are used [1].

Fig. 4 also shows the pressure histories with time at different locations. The incident, reflection, and transmission of pressure waves exist at the branched junction and in-phase and out-of-phase reflections occur at the closed end and the open end, respectively. Therefore, the flow pattern is changed consequently and both the supplier and collector flow types appear at the branched junction. The present calculation data shows a similar result to the ones obtained by the iterative calculation. Both calculated results agree well with the measurement data. The smooth change between different flow types is quite important for the stable numerical solution. Some differences of the phase between the calculated ones and measurement data for the long time history are due to the assumptions of a tiny internal volume within the junction and a constant friction coefficient [6]. Another reason may be that the real behaviour of pressure waves is not taken into account at the open end.

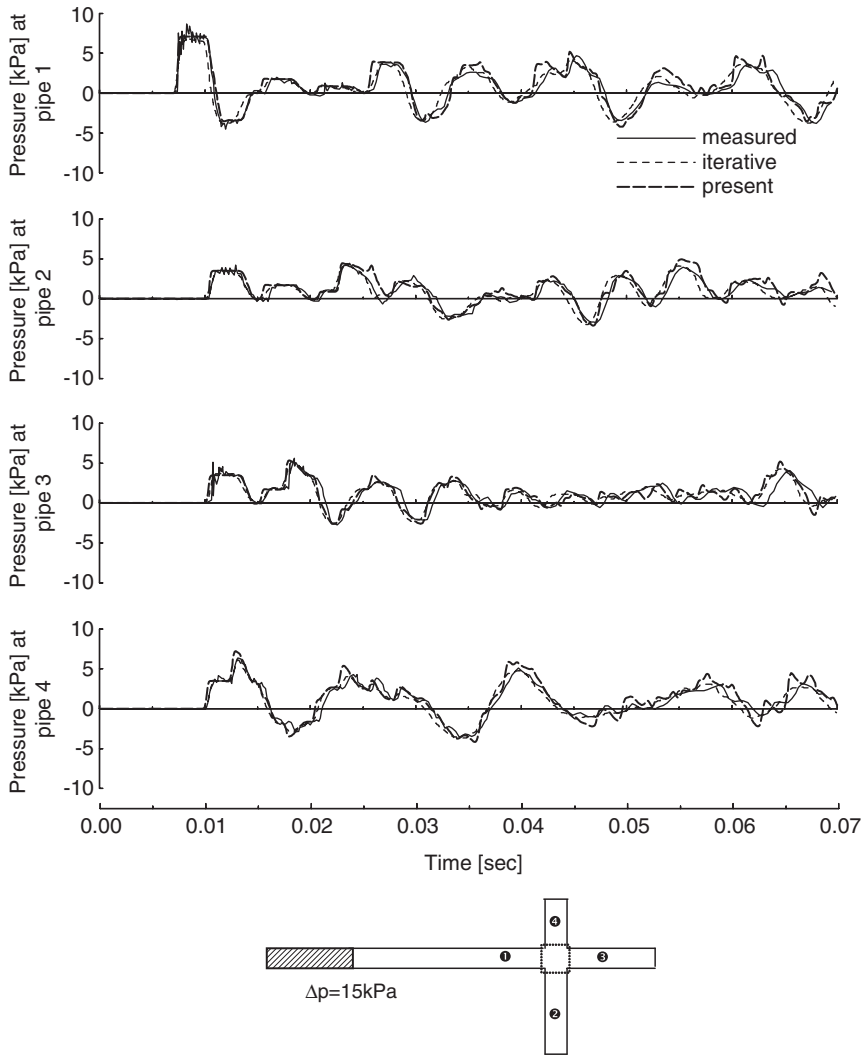

Fig. 5. Pressure history of the shock tube with a 4-branch junction.

Fig. 5 represents the case of the shock tube with a 4-branch junction, where the ends of all branch pipes are closed. More variations of pressure are shown. The calculated result agrees well with the measurement data, too.

3.2. Helmholtz resonator

For the second numerical validation, the calculation of sound attenuation in the Helmholtz resonator is considered. The schematic is shown in Fig. 6, where two microphones measure the upstream pressure signal within the pipe and the downstream pressure field. Onorati performed the measurement [7]. For an upstream boundary condition, a harmonic fluctuating pressure is imposed at the first grid point:

$$p = p_o + \Delta p \sin(2\pi f t), \tag{20}$$

where the amplitude Δp is kept at a small value ($\Delta p = 0.5\,\text{kPa}$). The subscript refers to the conditions in the ambient air.

For the boundary condition of sudden area change, the pressure recovery model for a sudden enlargement and isentropic pressure drop model for a sudden contraction are adopted [1]. The balance equations are

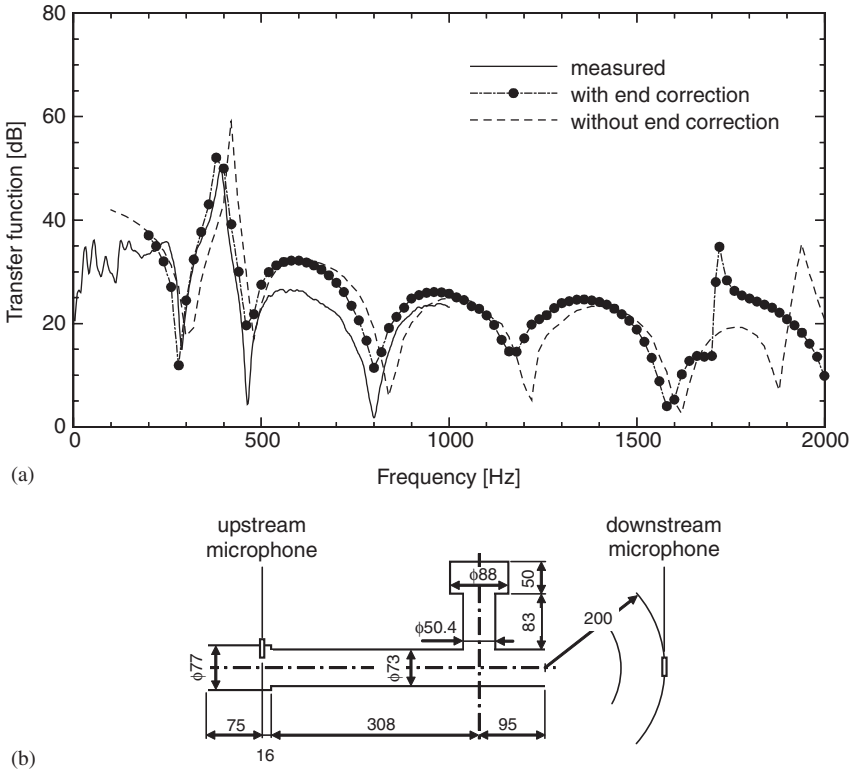

Fig. 6. Transfer function of a Helmholtz resonator.

transformed into quasi-linear equations by the similar manner of the present formulation of the branched junction. The radiated sound is obtained from the predicted velocity history at the open termination with the assumption of a simple monopole source, successfully applied in Refs. [7,12]:

$$p(t) = \frac{\rho_0 A}{4\pi r} + \frac{\mathrm{d}}{\mathrm{d}t} u(t - r/a_0), \tag{21}$$

where r is a distance from the open termination.

Fig. 6 also shows the comparison between the measured and calculated transfer functions, where the transfer function value is based on the rms values of the upstream oscillating pressure and the radiated sound pressure. The measured resonant frequencies are 287, 463 and 801 Hz. To improve the calculation results of wave interactions, end corrections are introduced at the open-end termination and sudden area change [7]. Some difference in magnitude and shift of frequency appear between inclusion and exclusion of the end corrections. With the end correction the calculated data agree well with the measured data. However, the agreement should be limited to the low-frequency range because of the original limitations of the one-dimensional flow calculation. The present approach has no difficulties of divergence and multiple solutions.

3.3. Internal combustion engine

In the one-dimensional gas dynamic calculation of internal combustion engines, branched junctions are frequently encountered. The boundary conditions at the junction are most important for both the accuracy of solution and the computing effort [13]. The robust, accurate, and fast present model, therefore, is appropriate for the calculation of breathing performance and radiated orifice noise of the internal combustion engines.

For the numerical test, a two-cylinder engine is considered. The schematic is shown in Fig. 7. In-cylinder condition is calculated from the first law of thermodynamics for an open system. The cylinder wall heat

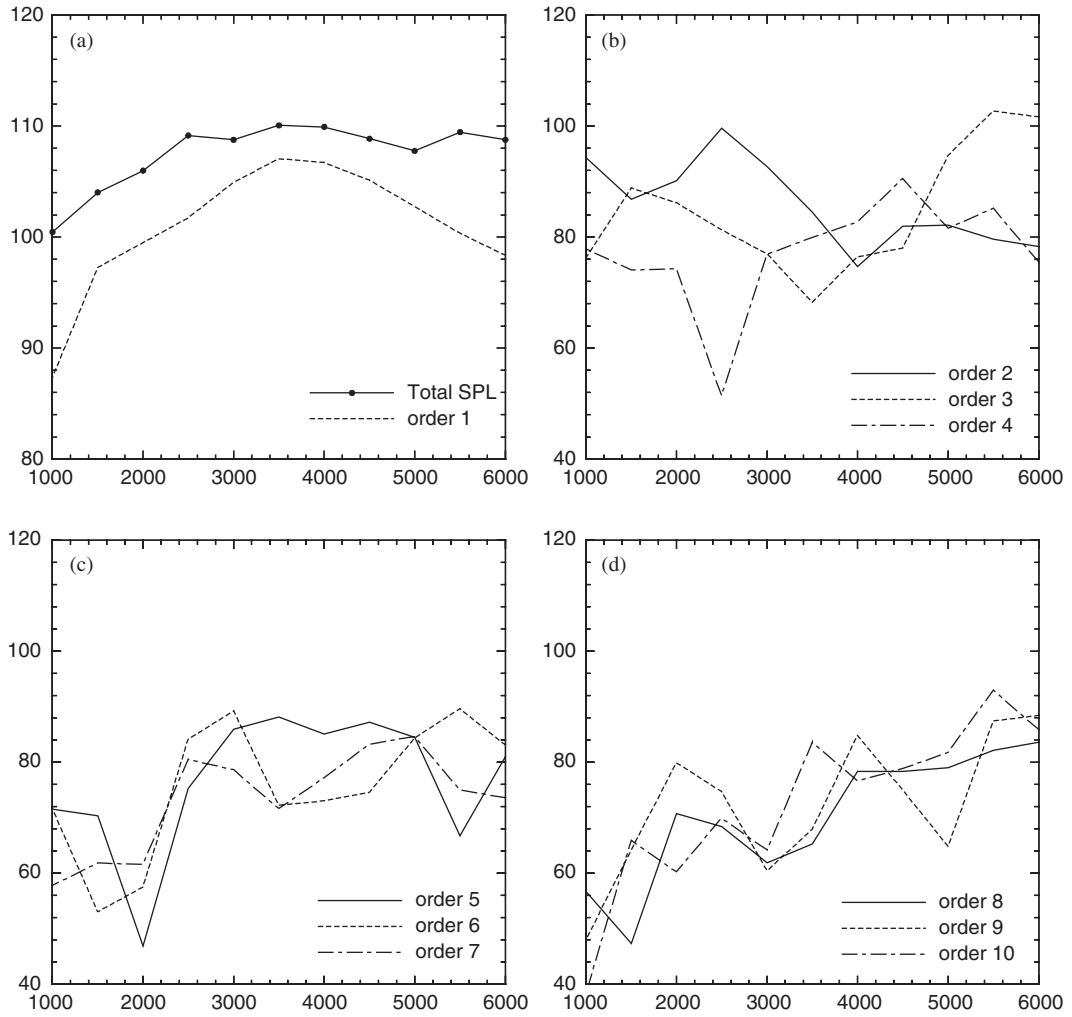

Fig. 7. Radiated intake noise of the 2-cylinder engine with an expansion chamber: (a) total sound pressure level and order 1 component; (b) order 2, 3, and 4 components; (c) order 5, 6, and 7 components; (d) order 8, 9, and 10 components.

transfer and heat release due to combustion are taken into account, too. The boundary condition for mass exchange through valves is based on a quasi-steady assumption with an empirical discharge coefficient [1].

Fig. 7 shows the ordered sound pressure level of intake orifice noise. The radiated sound is calculated by using Eq. (21). It can be observed that the order 2 frequency component (first harmonic of the firing frequency) and the order 3 component (second harmonic of the firing frequency) contribute to the peaks of total sound pressure level at 2500 and 5600 rev/min, respectively. In order to simulate the change of the radiated noise, Helmholtz resonator and quarter wave tube are attached to the intake system. The resonance frequencies of the components are 83.3 and 275 Hz, respectively. Fig. 8 shows the intake system configuration and the calculated radiated noise. Reduction of order 2 frequency component at 2500 rev/min and order 3 frequency component at 5500 rev/min are observed. The order 2 frequency at 2500 rev/min is equal to the order 1 frequency at 5000 rev/min. Therefore, the order 1 frequency component is also reduced at 5000 rev/min. Not only a drastic reduction of total sound pressure level but also rather less variation of each ordered frequency components are observed through the wide engine speed range.

Fig. 9 shows the comparisons of engine breathing performance and total sound pressure level. It is shown that the intake system configuration affects the engine performance as well as the radiated noise. The total

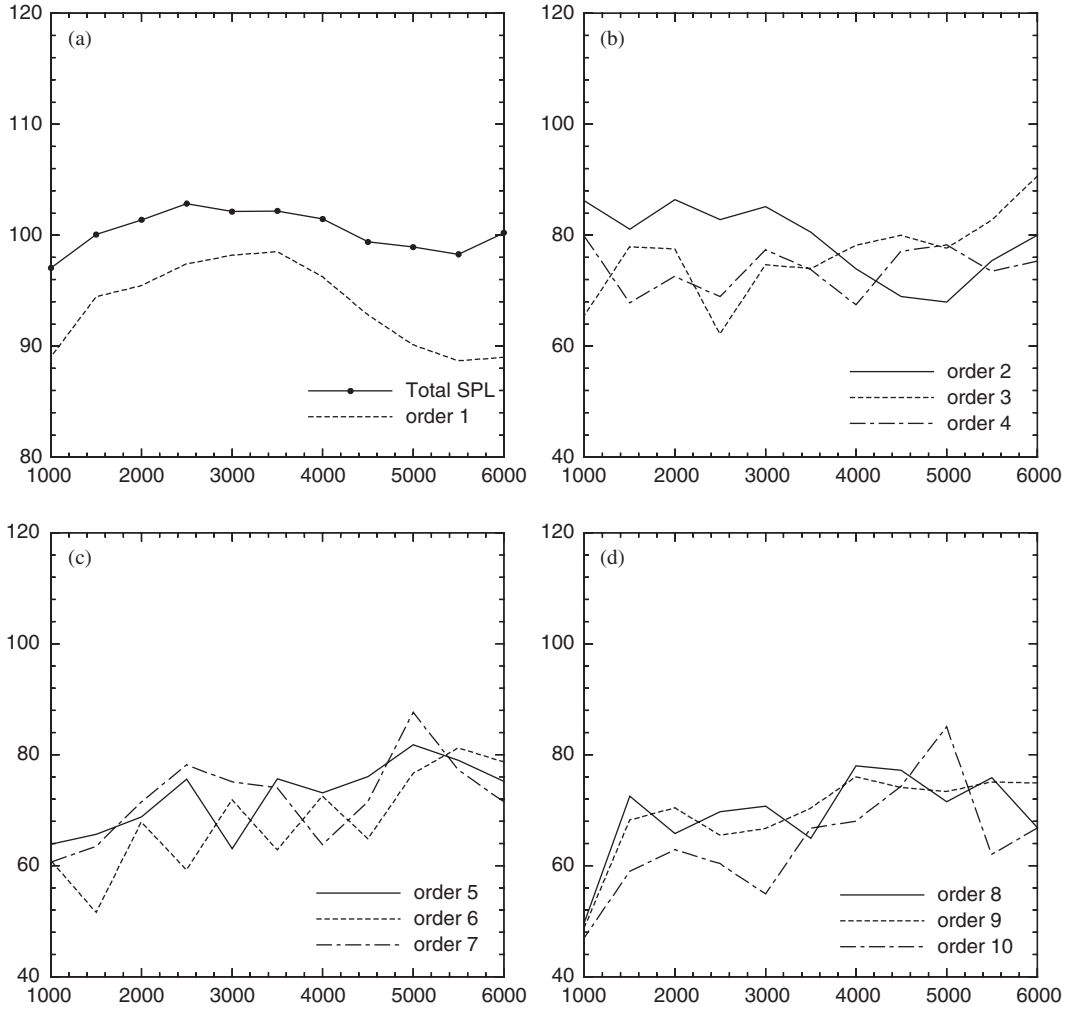

Fig. 8. Radiated intake noise of the 2-cylinder engine with expansion chamber, Helmholtz resonator and quarter wave tube: (a) total sound pressure level and order 1 component; (b) order 2, 3, and 4 components; (c) order 5, 6, and 7 components; (d) order 8, 9, and 10 components.

sound pressure level is reduced for overall engine speed and at the same time the breathing performance is also increased for some engine speed in this numerical simulation.

4. Conclusion

For the junction boundary in a pipe system, we need a set of balance equations and a characteristic information along with the boundary conditions at the end of each pipe. To obtain a well-posed problem, we reexamined the nonlinear balance equations of a general n-branch junction with pressure losses. We reformulated the balance equations into the closed system of quasi-linear equations. We used Thompson's boundary condition at each pipe to formulate a new balance equation of time-derivative forms. The balance equation at the junctions are simultaneous algebraic equations that are not coupled with the boundary condition of each pipe. For a case unbalance by numerical problems, we add some correction terms. We successfully applied the new mathematical model to shock tube with a branched junction and a Helmholtz resonator. The problems of divergence and multiple solutions are not shown, and the results agreed well with the previous iterative calculation and measurement data. The total sound pressure level and its order

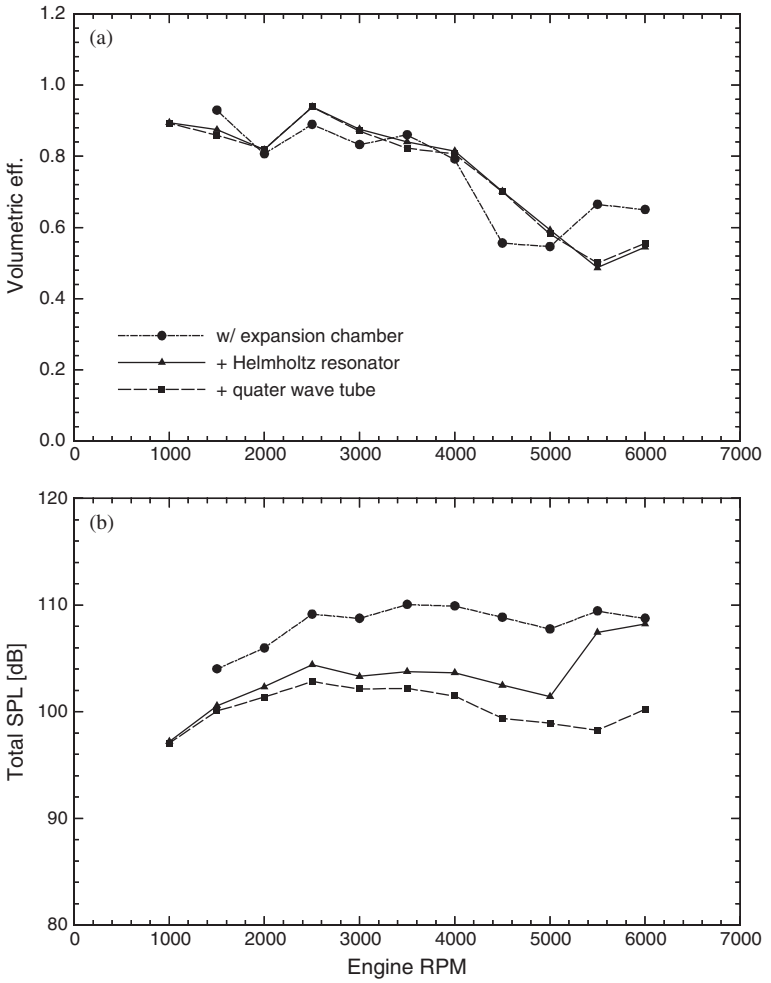

Fig. 9. Two-cylinder engine with a different intake configuration: (a) volumetric efficiency; (b) total sound pressure level.

components for a two-cylinder engine are simulated. Realistic predictions of the engine breathing performance and radiated orifice intake noise are obtained and the effects of acoustic components are also observed.

Appendix A. Characteristic boundary condition

Let us consider the conservative laws for the quasi-one-dimensional unsteady compressible perfect gas flows with wall friction and heat transfer in pipe as

$$\frac{\partial \mathbf{Q}}{\partial t}+\frac{\partial \mathbf{F}}{\partial x}+\mathbf{S}=\mathbf{0}. \tag{A.1}$$

Q, **F**, and **S** are column vectors of dimension three

$$\mathbf{Q}=\begin{bmatrix}\rho\\ \rho u\\ \rho e_o\end{bmatrix},\quad \mathbf{F}=\begin{bmatrix}\rho u\\ \rho u^2+p\\ \rho u h_o\end{bmatrix},\quad \mathbf{S}=\begin{bmatrix}\rho u\\ \rho u^2\\ \rho u h_o\end{bmatrix}\frac{1}{A}\frac{\mathrm{d}A}{\mathrm{d}x}+\begin{bmatrix}0\\ f\dfrac{\rho u^2}{2}\dfrac{u}{|u|}\dfrac{4}{D}\\ -\rho q\end{bmatrix}, \tag{A.2a,b,c}$$

where e_o is the internal energy, A the sectional area of pipe, D the diameter of pipe, f the wall friction factor, and q the wall heat loss per unit length.

Diagonalization of Eq. (A.1) is given by

$$\frac{\partial \mathbf{W}}{\partial t} + \Lambda \frac{\partial \mathbf{W}}{\partial x} + \mathbf{N} = \mathbf{0}, \tag{A.3}$$

where

$$\delta \mathbf{W} = \mathbf{P}^{-1}\delta \mathbf{Q} = \begin{bmatrix} \delta p - \rho a \delta u \\ a^2 \delta \rho - \delta p \\ \delta p + \rho a \delta u \end{bmatrix}, \tag{A.4}$$

$$\Lambda = \begin{bmatrix} \lambda_1 & 0 & 0 \\ 0 & \lambda_2 & 0 \\ 0 & 0 & \lambda_3 \end{bmatrix} = \begin{bmatrix} u-a & 0 & 0 \\ 0 & u & 0 \\ 0 & 0 & u+a \end{bmatrix} \tag{A.5}$$

and

$$\mathbf{N} = \mathbf{P}^{-1}\mathbf{S}, \tag{A.6}$$

where a is the speed of sound and $\mathbf{P}$ the transformation matrix.

Eq. (A.3) is a set of wave equations for waves with characteristic velocities λ_i corresponding to the original Eq. (A.1). Eigenvalues λ_1 and λ_3 are the velocities of sound waves propagating in the negative and positive direction. Eigenvalue λ_2 is the convection velocity of an entropy wave. The transformation matrix $\mathbf{P}$ can be found in Ref. [14]:

Following Thompson's characteristic approach [9], let us define the convection term in Eq. (A.3) as a column vector

$$\mathbf{L} \equiv \Lambda \frac{\partial \mathbf{W}}{\partial x}. \tag{A.7}$$

Thus, Eq. (A.3) may be written as

$$\frac{\partial \mathbf{W}}{\partial t} + \mathbf{L} + \mathbf{N} = \mathbf{0} \tag{A.8a}$$

or

$$\frac{\partial \mathbf{W}}{\partial t} = -R, \tag{A.8b}$$

where R is defined for the convenience of analysis.

The $\mathbf{N}$ in Eq. (A.8) is an inhomogeneous term, which does not contain derivatives of any components of $\mathbf{W}$. Therefore, the terms N_i may be evaluated just as constant terms. At a given location, the values of L_i are the time variations of wave amplitudes W_i.

Eq. (A.8b) may be rewritten as

$$\begin{aligned} &\frac{\partial p}{\partial t} - \rho a \frac{\partial u}{\partial t} = -R_1, \\ &a^2 \frac{\partial \rho}{\partial t} - \frac{\partial p}{\partial t} = -R_2, \\ &\frac{\partial p}{\partial t} + \rho a \frac{\partial u}{\partial t} = -R_3, \end{aligned} \tag{A.9a, b, c}$$

Eq. (A.9) can be arranged as

$$\begin{aligned} &\frac{\partial \rho}{\partial t} + \frac{1}{a^2}\left\{ R_2 + \frac{1}{2}(R_3 + R_1) \right\} = 0, \\ &\frac{\partial p}{\partial t} + \frac{1}{2}(R_3 + R_1) = 0, \\ &\frac{\partial u}{\partial t} + \frac{1}{2\rho a}(R_3 - R_1) = 0. \end{aligned} \tag{A.10a, b, c}$$

In general, the original Eq. (A.1) contains eigenvalues of both signs at the boundary, so that difficulty arises in the implementation of boundary conditions. However, one can consider each wave separately by using the characteristic Eq. (A.8) or (A.10). To apply the boundary conditions, it is first necessary to determine which characteristic waves are incoming or outgoing. The behaviour of the waves moving from the interior of pipe to boundary is completely determined from Eq. (A.7) using one-sided difference approximations.

In the case of flow moving from the interior to the boundary, the outgoing waves L_1 and L_2 can be directly obtained at $x = x_0$ (the boundary) with a second order accuracy based on a uniform space discretization:

$$L_1 = \lambda_1\left(\frac{\partial p}{\partial x} - \rho a\frac{\partial u}{\partial x}\right) \approx (u_0 - a_0)\left(\frac{-3p_0 + 4p_1 - p_2}{2\Delta x_0} - \rho_0 a_0\frac{-3u_0 + 4u_1 - u_2}{2\Delta x_0}\right),$$

$$L_2 = \lambda_2\left(a^2\frac{\partial \rho}{\partial x} - \frac{\partial p}{\partial x}\right) \approx u_0\left(a_0^2\frac{-3\rho_0 + 4\rho_1 - \rho_2}{2\Delta x_0} - \frac{-3p_0 + 4p_1 - p_2}{2\Delta x_0}\right), \quad \text{(A.11a, b)}$$

where the subscripts denote node points except for L and λ.

One of the physical boundary conditions, imposing a constant pressure on boundary for example, requires setting $L_3 = -L_1$ to satisfy Eq. (A.10b) and all values of L_i are determined (the inhomogeneous terms N_i assumed to be zero). Eq. (A.10) provides the time derivatives of boundary values based on the current solution. The coefficients of R_i in Eq. (A.10) are assumed to be locally constant and the integration of Eq. (A.10) gives the next time level boundary values.

References

[1] R.S. Benson, *The Thermodynamics and Gas Dynamics of Internal-Combustion Engines*, Vol. 1, Clarendon Press, Oxford, 1982.

[2] J.F. Bingham, G.P. Blair, An improved branched pipe model for multi-cylinder automotive engine calculations, *Proceedings of the Institution of Mechanical Engineers* 199 (D1) (1985) 65–77.

[3] J.M. Corberan, A new constant pressure model for *n*-branch junction, *Journal of Automobile Engineering, Proceedings of the Institution of Mechanical Engineers, Part D* 206 (1992) 117–123.

[4] T. Bulaty, M. Widenhorn, Unsteady flow calculation of sophisticated exhaust systems using a multibranch junction model, *Transactions of the ASME, Journal of Engineering for Gas Turbines and Power* 115 (1993) 756–760.

[5] M.J.P. William–Louis, C. Tournier, Calculation of pressure wave propagation through a tube junction, *Proceedings of the Institution of the Mechanical Engineers, Part C, Journal of Mechanical Engineering Science* 210 (1996) 239–244.

[6] M.J.P. William–Louis, A. Ould-El-Hadrami, C. Tournier, On the calculation of the unsteady compressible flow through an *n*-branch junction, *Proceedings of the Institution of the Mechanical Engineers, Part C, Journal of Mechanical Engineering Science* 212 (1998) 49–56.

[7] A. Onorati, Prediction of the acoustical performances of muffling pipe systems by the method of characteristics, *Journal of Sound and Vibration* 171 (1994) 369–395.

[8] G. Engl, The modelling and numerical simulation of gas flow networks, *Numerische Mathematik* 72 (1996) 349–366.

[9] K.W. Thompson, Time dependent boundary conditions for hyperbolic systems, *Journal of Computational Physics* 68 (1987) 1–24.

[10] R. Fleck, P. Long, D. Thornhill, G. Blair, Validation of a non-isentropic, pressure loss, branched pipe junction model, *SAE Paper No. 982055*, 1998.

[11] D.K. Ko, D.J. Lee, Third order, modified flux approach type essentially nonoscillating schemes for wave equations, *AIAA Journal* 37 (3) (1999) 384–385.

[12] F. Payri, A.J. Torregrosa, M.D. Chust, Application of MacCormack schemes to I.C. engine exhaust noise prediction, *Journal of Sound and Vibration* 195 (1996) 757–773.

[13] T. Bulaty, H. Niessner, Calculation of 1-D unsteady flows in pipe systems of I.C. engines, *Transactions of the ASME, Journal of Fluids Engineering* 107 (1985) 407–412.

[14] C. Hirsch, *Numerical Computation of Internal and External Flows*, Vol. 2, Wiley, New York, 1990.